Designing ALPES: an Adaptable Lab for Plasma Experiments in Stellarators at university scale

E.M. Steinwender[1], C.G. Albert[1], G. Birkenmeier[2,3], D. Mendonça[2], M. Narnhofer[1], N. Oberth[1], M. Oblak[1], M. Rosenthal[2], R. Schennach[1,4], J. Schilling[5], U. Stroth[2,3], M. Tritthart[1], ALPES Team

[1] *Fusion@ÖAW, Technische Universität Graz, Rechbauerstraße 12, 8010 Graz, Austria*

[2] *Technical University of Munich, TUM School of Natural Sciences, Physics Department, James-Franck-Str. 1, 85748 Garching, Germany*

[3] *Max Planck Institute for Plasma Physics, Boltzmannstraße 2, 85748 Garching, Germany*

[4] *Institute of Solid State Physics, TU Graz, Petersgasse 16, 8010 Graz, Austria*

[5] *Proxima Fusion GmbH, Flößergasse 2, 81369 Munich, Germany*

We present the design of a tabletop compact stellarator, called ALPES [1], with the focus on flexibility with respect to interchangeable coil configurations and extensibility. The work is the result of the joint course *Fusion Reactor Design* of TU Graz, TU Munich and Proxima Fusion with support from the Max-Planck-Institute for Plasma Physics. The following requirements have been imposed: (a) maximum size of 190 cm x 90 cm, (b) low aspect ratio of the plasma of approximately 4, (c) large volume, and (d) simple coil concept. The design is based on an existing configuration from the QUASR database [1].

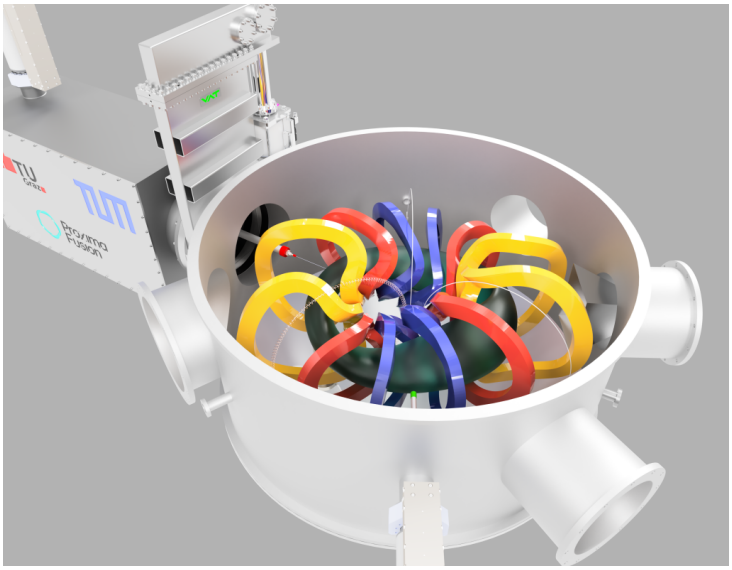

Figure 1: **3D model of the complete setup:** Vacuum vessel containing the coils and plasma to the right front together with box for diagnostics and manipulators on the top left.

The configuration consists of 12 coils of three different types, and a minimum inter-coil distance of 15 cm, which allows placement and casing of the coils with sufficient spacing. The

[1] ALPES = **A**daptable **L**ab for **P**lasma **E**xperiments in **S**tellarators at university scale

plasma has a major radius of 1 m and a minor radius of 0.25 m with a plasma volume of 1.2 m^3. The robustness of the nested magnetic flux surfaces with respect to the manufacturing tolerances was tested with the *SIMSOPT* [7] and *STELLOPT* [8] codes, comparing the effects of shifted and scaled coils to the base configuration using Poincaré plots. These reveal slight island formation at a shift of 1 cm for a single coil. Alpha particle confinement of an upscaled device of W7-X size was calculated in the code *SIMPLE* [9][10] to be around 70 %. Comparing Larmor radius and device size, electron orbits in ALPES can act as a scale model for alpha orbits in a reactor.

The **main vacuum chamber** (Figure 1) has a diameter of 1.6 m and a height of 0.6 m. The material of the recipient is a non-magnetic austhenitic stainless steel, grade 316 L, with a wall thickness of 10 mm, which ensures sufficient protection against X-ray and microwave radiation. The quartz-glass windows with removable lead plates have likewise a thickness of 10 mm and a diameter of 100 mm. It houses ports for coil mounts, heating and diagnostics. The dome-shaped top and bottom guarantee sufficient space, transport flexibility and rigidity during evacuation. A universal flange size of *DN 320 ISO-F* is used, which is suitable for the turbomolecular pump (TMP), and by using adapters, different devices can be attached for future upgrades without reducing the quality of the chamber or increasing its price. The TMP is supported by a roughing pump. The flanges for the combined Pirani-Bayard-Alpert pressure measurement and the quadrupole spectrometer for residual gas analysis are of different sizes. The support structure, positioned under and mounted to the lateral surfaces of the chamber, has a total load-bearing capacity of 15 t. Heat and electrical insulation are provided by Kapton.

The **magnetic field** of B= 87.5 mT is generated by 12 water cooled **coils** of three different types (Figure 2a). The coil-system is designed to minimize the deviation from the symmetric field (comparison via Poincaré-plots) and to withstand a maximum temperature of 200°C. These temperatures can occur within the bake-out procedure used to improve vacuum quality. Each coil uses a double pancake design and has a total cross section of 44 mm x 67 mm. It consists of hollow copper conductors to enable active water cooling. The windings are held together and insulated from each other through a fiberglass reinforced epoxy composite with a thickness of approximately 0.5 mm to 1 mm. In order to prevent outgassing from the epoxy into the vacuum, each coil is encapsulated in a 2 mm thick stainless steel casing.

For **diagnosing plasma** parameters, an essential set of diagnostics is introduced. An interferometer measures the phase shift of a wave as it passes through the magnetized plasma, which is related to the line-integrated electron density. The magnetic diagnostics consists of two diamagnetic coils for the poloidal and one Rogowski coil for the toroidal current including lock-in amplifiers, low- and high band passes and D/A converters to filter out the noise and amplify the

current signal. A Langmuir probe is used to determine the I-V characteristic curve, which has the advantage of being able to reach and determine every point in the plasma cross-section due to the 2-dimensional movement. Attention was paid to a plug-in probe holder so that the probe tips can be exchanged for other holders.

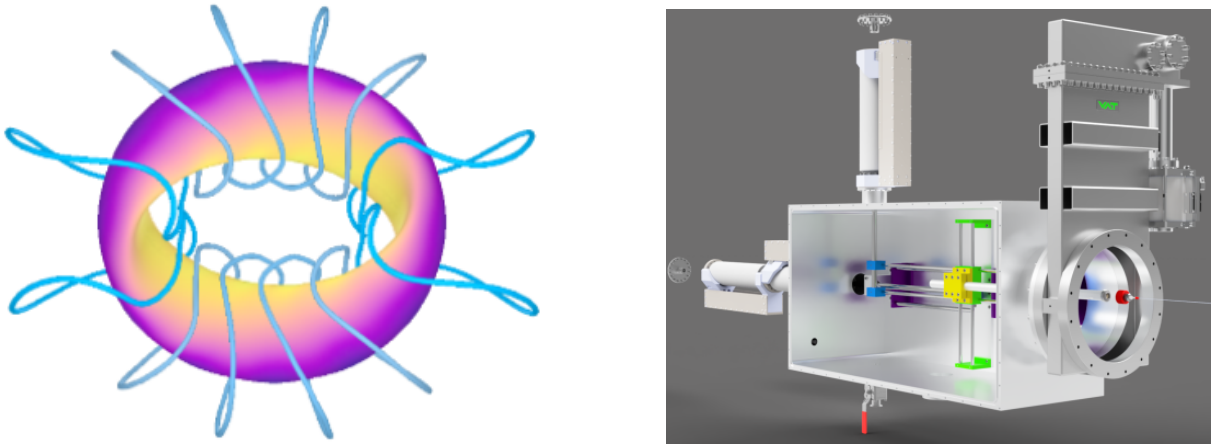

(a) (b)

Figure 2: **a) Coil configuration** taken from [1] **b) Diagnostics:** Vacuum box of the 2D-manipulator with the probe-holder and Langmuir-probe tip inlcuding an UHV-gate.

A **microwave system** operating at 2.45 GHz is used to generate plasma and achieve experimental temperatures. This frequency matches the electron cyclotron resonance frequency (ECRF) at the design magnetic field $B = 87.5\,\mathrm{mT}$, which is important for plasma startup. After that the plasma heating will take place near the upper hybrid resonance at the plasma edge [5]. The 1D simulation of steady-state plasma profiles (Figure 3) was performed with the heating peaking near the edge at $r = 0.066\,\mathrm{m}$. Assuming fixed diffusivities, density scales with heating power, while temperature remains relatively constant due to a balance between ionization and diffusion.

It should, however, be noted that these profiles depend strongly on transport coefficients, which were assumed to be similar to those of TJ-K [4]. Near the edge, where the particle density reaches $7.4 \times 10^{16}\,\mathrm{m}^{-3}$, the plasma frequency $\omega_\mathrm{p} = 2.45\,\mathrm{GHz}$ causes O-wave reflection [3]. Initial heating, therefore, occurs via resonance at the upper-hybrid frequency $\omega_\mathrm{UH} = \sqrt{\omega_\mathrm{C}^2 + \omega_\mathrm{p}^2}$ ($\omega_\mathrm{C} < 2.45\,\mathrm{GHz}$ at $B < 87.5\,\mathrm{mT}$, in low field side) [6]. As density rises, ω_UH resonance shifts to the edge. Core heating can then also utilize Bernstein waves (B-waves) at the ECRF or its harmonics. This requires an adjustable antenna angle via a flexible waveguide or, in advanced stages, a phased array antenna operating at a higher harmonic of the ECRF [5].

Data availability

Design material and data are available as open source [2] for re-use and further development.

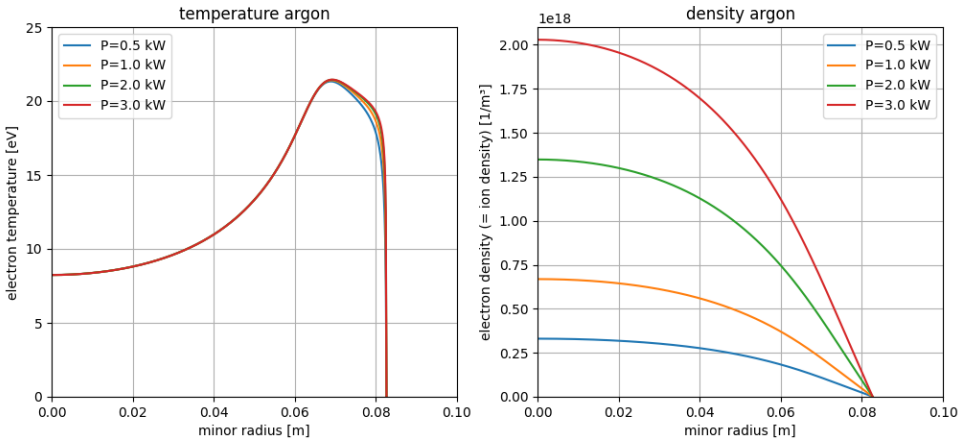

Figure 3: **Temperature and density profiles** for different heating powers (P). The boundary conditions are of: zero gradient at the center ($r = 0$); fixed value at the edge ($r = \max$).

Acknowledgement

This work has been carried out within the framework of the EUROfusion Consortium, funded by the European Union via the Euratom Research and Training Programme (Grant Agreement No 101052200 — EUROfusion). Views and opinions expressed are however those of the author(s) only and do not necessarily reflect those of the European Union or the European Commission. Neither the European Union nor the European Commission can be held responsible for them. We thank Max-Planck-Institute for Plasma Physics, in particular the team of Eve Stenson. We gratefully acknowledge support from NAWI Graz, Proxima Fusion, and TU Graz via the seed funding and Joint Course initiatives.

References

[1] A. Giuliani. Flatiron Institute QUAsi-symmetric Stellarator Repository. https://quasr.flatironinstitute.org/model/0021326, accessed Jan 10, 2025.

[2] Fusion Reactor Design 2024 Git repository. https://github.com/itpplasma/reactor24, accessed Jan 10, 2025.

[3] U. Stroth. Plasmaphysik. Berlin, Heidelberg: Springer Berlin Heidelberg, 2018. ISBN: 978-3-662-55235-3. https://doi.org/10.1007/978-3-662-55236-0

[4] G. Birkenmeier. Experiments and Modeling of Transport Processes in Toroidal Plasmas. Diploma Thesis: Universität Stuttgart (2008)

[5] A. Köhn et al. **55**, 014010 (2012) https://doi.org/10.1088/0741-3335/55/1/014010

[6] A. Köhn et al. Plasma Phys. Control. Fusion, **52**, 035003 (2010) https://doi.org/10.1088/0741-3335/52/3/035003

[7] M. Landreman, B. Medasani, F. Wechsung, A. Giuliani, R. Jorge, and C. Zhu, *J. Open Source Software*, vol. 6, p. 3525, 2021. DOI: 10.21105/joss.03525

[8] S. Lazerson, J. Schmitt, C. Zhu, J. Breslau, and all STELLOPT Developers, *STELLOPT* [Computer Software], May 2020. Available at: https://doi.org/10.11578/dc.20180627.6

[9] C. G. Albert, S. V. Kasilov, and W. Kernbichler, *J. Plasma Physics*, vol. 86, p. 815860201, 2020. DOI: 10.1017/S0022377820000203

[10] C. G. Albert, S. V. Kasilov, and W. Kernbichler, *J. Comp. Phys.*, vol. 403, p. 109065, 2020. DOI: 10.1016/j.jcp.2019.109065